Surface plasmon subwavelength optics

William L. Barnes[1], Alain Dereux[2] & Thomas W. Ebbesen[3]

[1]*School of Physics, University of Exeter, EX4 4QL, UK (e-mail: w.l.barnes@ex.ac.uk)*
[2]*Laboratoire de Physique, Université de Bourgogne, BP 47870, F-21078 Dijon, France (adereux@u-bourgogne.fr)*
[3]*ISIS, Université Louis Pasteur, BP 70028, F-67083, Strasbourg Cedex, France (e-mail: ebbesen@isis-ulp.org)*

Surface plasmons are waves that propagate along the surface of a conductor. By altering the structure of a metal's surface, the properties of surface plasmons—in particular their interaction with light—can be tailored, which offers the potential for developing new types of photonic device. This could lead to miniaturized photonic circuits with length scales that are much smaller than those currently achieved. Surface plasmons are being explored for their potential in subwavelength optics, data storage, light generation, microscopy and bio-photonics.

Surface plasmons (SPs) are of interest to a wide spectrum of scientists, ranging from physicists, chemists and materials scientists to biologists. Renewed interest in SPs comes from recent advances that allow metals to be structured and characterized on the nanometre scale. This in turn has enabled us to control SP properties to reveal new aspects of their underlying science and to tailor them for specific applications. For instance, SPs are being explored for their potential in optics, magneto-optic data storage, microscopy and solar cells, as well as being used to construct sensors for detecting biologically interesting molecules.

SPs were widely recognized in the field of surface science following the pioneering work of Ritchie in the 1950s (ref. 1). SPs are waves that propagate along the surface of a conductor, usually a metal. These are essentially light waves that are trapped on the surface because of their interaction with the free electrons of the conductor (strictly speaking, they should be called surface plasmon polaritons to reflect this hybrid nature[2]). In this interaction, the free electrons respond collectively by oscillating in resonance with the light wave. The resonant interaction between the surface charge oscillation and the electromagnetic field of the light constitutes the SP and gives rise to its unique properties.

For researchers in the field of optics, one of the most attractive aspects of SPs is the way in which they help us to concentrate and channel light using subwavelength structures. This could lead to miniaturized photonic circuits with length scales much smaller than those currently achieved[3,4]. Such a circuit would first convert light into SPs, which would then propagate and be processed by logic elements, before being converted back into light. To build such a circuit one would require a variety of components: waveguides, switches, couplers and so on. Currently much effort is being devoted to developing such SP devices; one example is the 40 nm thick gold stripe that acts as a waveguide for SPs in Fig. 1. An appealing feature is that, when embedded in dielectric materials, the circuitry used to propagate SPs can also be used to carry electrical signals. Developments such as this raise the prospect of a new branch of photonics using SPs, sometimes called plasmonics.

The use of SPs to help us concentrate light in subwavelength structures stems from the different (relative) permittivities, ε, of the metals and the surrounding non-conducting media. (ε is the square of the complex index of refraction.) Concentrating light in this way leads to an electric field enhancement that can be used to manipulate light–matter interactions and boost non-linear phenomena. For example, metallic structures much smaller than the wavelength of light are vital for the massive signal enhancement achieved in surface-enhanced Raman spectroscopy (SERS)—a technique that can now detect a single molecule[5,6]. Furthermore, the enhanced field associated with SPs makes them suitable for use as sensors, and commercial systems have already been developed for sensing biomolecules. SP-based sensing applications and SERS will not be discussed further here because they are covered by other reviews[7,8].

Here we provide an overview of the properties of SPs and indicate why they are being considered for subwavelength optics. We examine how their propagation can be manipulated and discuss some of the optical components that have so far been demonstrated. We conclude by highlighting the practical potential of this field and indicate just how much work remains to be done for that potential to be realized.

Coupling to surface plasmons

The interaction between the surface charges and the electromagnetic field that constitutes the SP has two consequences (see Box 1). First, the interaction between the surface charge density and the electromagnetic field results in the momentum of the SP mode, $\hbar k_{SP}$, being greater than that of a free-space photon of the same frequency, $\hbar k_0$. ($k_0 = \omega/c$ is the free-space wavevector.) Solving Maxwell's equations under the appropriate boundary conditions yields the SP dispersion relation[9], that is, the frequency-dependent SP wave-vector, k_{SP},

$$k_{SP} = k_0 \sqrt{\frac{\varepsilon_d \varepsilon_m}{\varepsilon_d + \varepsilon_m}} \qquad (1)$$

The frequency-dependent permittivity of the metal, ε_m, and the dielectric material, ε_d, must have opposite signs if SPs are to be possible at such an interface. This condition is satisfied for metals because ε_m is both negative and complex (the latter corresponding to absorption in the metal). As an example, using equation (1), the SP wavevector for a silver–air interface in the red part of the visible spectrum is found to be $k_{SP} \cong 1.03.k_0$. This increase in momentum is associated with the binding of the SP to the surface, and the resulting momentum mismatch between light and SPs of the same frequency must be bridged if light is to be used to generate SPs.

The second consequence of the interaction between the surface charges and the electromagnetic field is that, in contrast to the propagating nature of SPs along the surface, the field perpendicular to the surface decays exponentially with distance from the surface. The field in this perpendicular direction is said to be evanescent or near field in nature and is a consequence of the bound, non-radiative nature of SPs, which prevents power from propagating away from the surface.

There are three main techniques by which the missing momentum can be provided. The first makes use of prism coupling to enhance the momentum of the incident light[10,11]. The second involves scattering from a topological defect on the surface, such as a subwavelength protrusion or hole, which provides a convenient way to generate SPs locally[3,12]. The third makes use of a periodic corrugation in the metal's surface[13]. Indeed, over 100 years ago, Wood[14] reported anomalous behaviour in the diffraction of light by metallic diffraction gratings—some of these phenomena are now known to arise from coupling to SPs. The diffraction (scattering) of light by a metallic diffraction grating allows incident light to be momentum matched and thus coupled to SPs[15]. Importantly the reverse process also allows the otherwise non-radiative SP mode to couple with light in a controlled way with good efficiency[16,17], which is vital if SP-based photonic circuits are to be developed.

Surface plasmon propagation

Once light has been converted into an SP mode on a flat metal surface it will propagate but will gradually attenuate owing to losses arising from absorption in the metal. This attenuation depends on the dielectric function of the metal at the oscillation frequency of the SP. The propagation length, δ_{SP}, can be found by seeking the imaginary part, k''_{SP}, of the complex surface plasmon wavevector, $k_{SP} = k'_{SP} + ik''_{SP}$, from the SP dispersion equation (1) (ref. 15),

$$\delta_{SP} = \frac{1}{2k''_{SP}} = \frac{c}{\omega}\left(\frac{\varepsilon'_m + \varepsilon_d}{\varepsilon'_m \varepsilon_d}\right)^{\frac{3}{2}} \frac{(\varepsilon'_m)^2}{\varepsilon''_m} \qquad (2)$$

where ε'_m and ε''_m are the real and imaginary parts of the dielectric function of the metal, that is, $\varepsilon_m = \varepsilon'_m + i\varepsilon''_m$. Silver is the metal with the lowest losses in the visible spectrum: propagation distances are typically in the range 10–100 μm, increasing towards 1 mm as one moves into the 1.5 μm near-infrared telecom band (see Box 2). In the past, absorption by the metal was seen as such a significant problem that SPs were not considered viable for photonic elements; the SP propagation length was smaller than the size of components at that time. This view is now changing thanks primarily to recent demonstrations of SP-based components that are significantly smaller than the propagation length[18]. Such developments open the way to integrate many SP-based devices into circuits before propagation losses become too significant.

In addition to dealing with the problem of loss owing to absorption in the metal, there is another key loss mechanism that must be considered: unwanted coupling to radiation. To build SP-based circuits one will need components that convert one SP mode into another, for example, a switch to re-route SPs without scattering the SP mode in such a way as to lose its energy to freely propagating light.

Surface plasmon band structure and periodic surfaces

One of the key developments in photonics in the past 15 years has been that of photonic bandgap (PBG) materials. These synthetic materials use wavelength-scale periodic structures to manipulate the interaction between light and matter so as to build new photonic structures—a good example being that of the photonic crystal fibre[19]. These developments have been predominantly made in periodically structured insulating and semiconducting materials. By making use of SPs, metals too can be used as PBG materials, this time in the form of photonic surfaces[20].

The nature of SPs changes when they propagate on metal surfaces that are periodically textured on the scale of the wavelength of light.

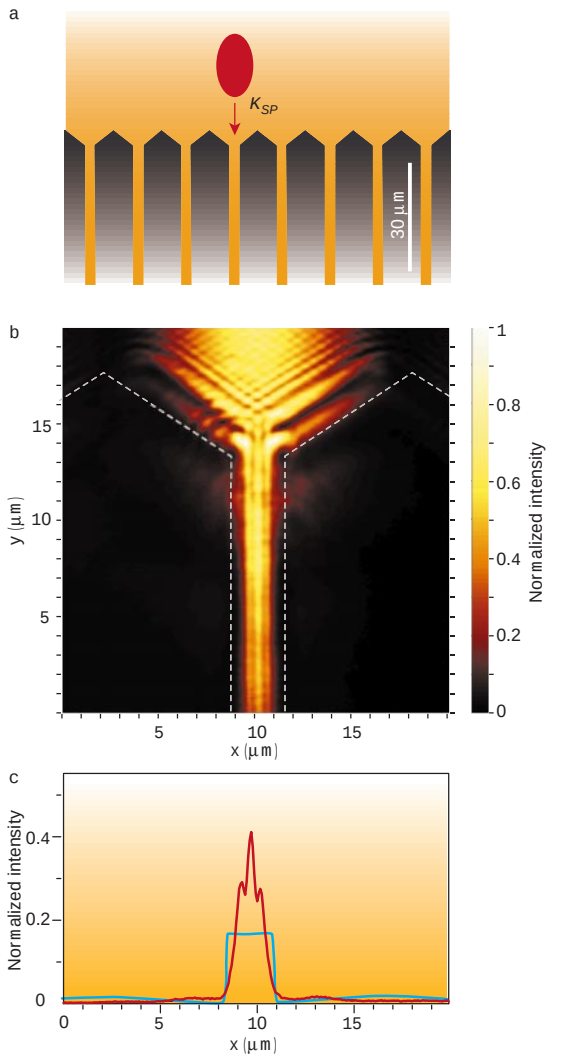

Figure 1 An SP waveguide. **a**, a scanning electron micrograph image of a 40 nm thick, 2.5 μm wide gold stripe lying on a glass substrate (courtesy of J. C. Weeber, Université de Bourgogne, France). **b**, The optical functionality of the stripe visualized by PSTM; an extended SP, launched on the larger area by a spot (indicated by the red ellipse) generated by total internal reflection illumination (wavelength=800 nm) through the substrate, is used to excite one of the stripe's SP eigen modes featuring three maxima. The photon scanning tunnelling microscopy (PSTM) image demonstrates that SPs are bound to the metal. **c**, A cross-section across the stripe shows that this mode is much better confined to the guiding material (indicated by the AFM topology—pale blue line) sustaining the mode than would be the case in dielectric-based waveguides. Not only the height of the guide but also the square root of the waveguide cross-section features a subwavelength size, underlining the fact that the SP mode is essentially bound to the metal surface rather than being a standing wave confined inside the metal volume.

When the period of the nanostructure is half that of the effective wavelength of the SP mode, scattering may lead to the formation of SP standing waves and the opening of an SP stop band[21] (see Box 3). When the surface is modulated in both in-plane directions, for example by a periodic array of bumps, SP modes may be prevented from travelling in any in-plane direction, thus leading to a full PBG for SP modes[20,22] (Fig. 2). Fig. 2 provides a nice demonstration of how the problems associated with absorption by the metal can be overcome. It shows that, although finite, the SP propagation length is more than enough to allow the SP to

Box 1
Surface plasmon basics

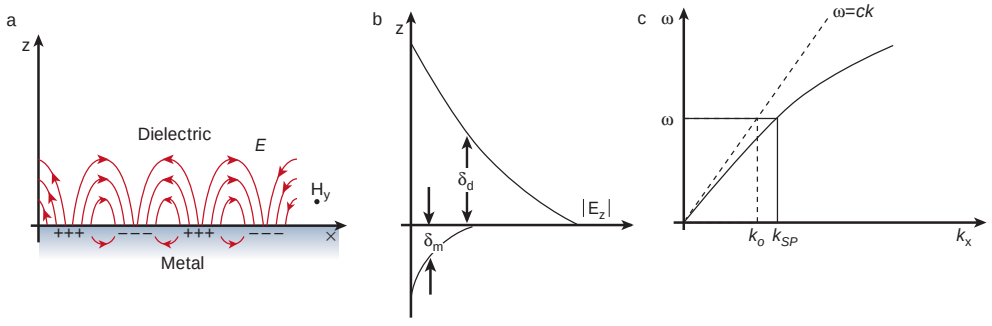

SPs at the interface between a metal and a dielectric material have a combined electromagnetic wave and surface charge character as shown in **a**. They are transverse magnetic in character (**H** is in the y direction), and the generation of surface charge requires an electric field normal to the surface. This combined character also leads to the field component perpendicular to the surface being enhanced near the surface and decaying exponentially with distance away from it (**b**). The field in this perpendicular direction is said to be evanescent, reflecting the bound, non-radiative nature of SPs, and prevents power from propagating away from the surface. In the dielectric medium above the metal, typically air or glass, the decay length of the field, δ_d, is of the order of half the wavelength of light involved, whereas the decay length into the metal, δ_m, is determined by the skin depth. **c**, The dispersion curve for a SP mode shows the momentum mismatch problem that must be overcome in order to couple light and SP modes together, with the SP mode always lying beyond the light line, that is, it has greater momentum ($\hbar k_{SP}$) than a free space photon ($\hbar k_0$) of the same frequency ω.

experience many periods of the textured surface and thus display the PBG phenomenon. We also note with interest that recent developments in the fabrication of periodic nanostructures via self-assembly offer the prospect of easily producing SP PBG substrates to act as photonic substrates on which to define SP photonic circuits.

At frequencies within a bandgap, the density of SP modes is zero—no SP modes can be supported. However, at the band edges, the SP mode dispersion is flat and the associated density of SP modes is high, corresponding to a high field enhancement close to the metal surface. Further, the nature of this flat band means that such modes can be excited by light that is incident over a wide range of angles, making them good candidates for frequency-selective surfaces. Flat bands are also associated with the localized SP modes of metallic nanoparticles[23,24]. The frequency and width of these modes are determined by the particle's shape, material, size and environment[23,25,26], and for this reason they are being pursued as tags for biosensing[27,28] and as substrates for SERS[29] and potentially as aerials for fluorophores[30,31]. The interaction between two or more nanoparticles can lead to still further levels of field enhancement[32–34], with even more dramatic effects associated with hot spots in random structures[35].

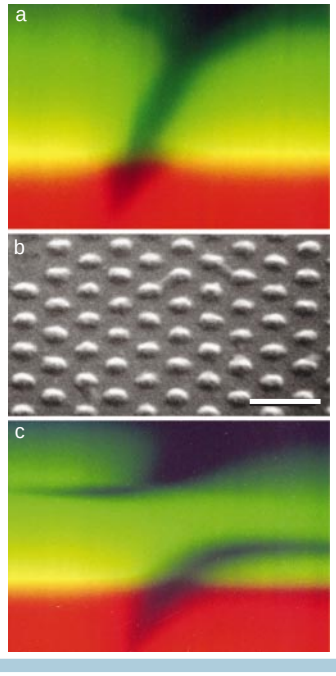

Figure 2 SP photonic bandgap. The SP dispersion curve shown in Box 1 was directly imaged using a modified prism coupling technique. **a**, The dispersion curve (here shown as inverse wavelength versus angle) for a flat surface is shown in the upper picture; here dark regions correspond to coupling of incident light to the SP mode, and the colours are produced on a photographic film by the wavelength of the light used. **b**, If the metal surface is textured with a two-dimensional pattern of bumps on an appropriate length scale (roughly half the wavelength of light) as shown in this SEM, a bandgap is introduced into the dispersion curve of the associated SP modes. Bar, 0.7 μm. **c**, The bandgap is clearly seen in the lower picture where there is a spectral region in which no SP mode (as indicated by the dark regions) exists. Also note the distortion of the SP mode and the edges of the bandgap.

Mapping surface plasmons and developing components

The properties of SP devices are intimately linked to the activity and the distribution of SPs on the metal surface. Much is still not known about the relationship between surface topology and the nature of the SP modes, and so a more detailed study of the details of this SP activity is vital. Because of the way SPs are confined to the surface and because of the subwavelength nature of the structures and fields involved, one cannot rely on traditional far-field techniques. Instead near-field techniques[3,36] such as photon scanning tunnelling microscopy (PSTM) are typically employed to map the fields on the metal surface, for example, those of the SP waveguide in Fig. 1. A PSTM is basically a collection mode scanning near-field optical microscope where the sample lies on a glass prism, which enables one to shine light in total internal reflection. The nanometre size tip, mostly obtained by pulling an optical fibre, which may eventually be coated with a metal, frustrates the total reflection when scanning close to the surface and thereby maps the near-field intensities.

Surprisingly, as we enhance the capabilities of near-field techniques further to map the SP fields into the subwavelength regime we come up against an interesting variant of Heisenberg's uncertainty principle. Applied to the optical field, this principle says that we can only measure the electric (E) or the magnetic field (H) with accuracy when the volume δl^3 in which they are contained is significantly smaller than the wavelength of light in all three spatial dimensions. More precisely, Heisenberg's uncertainty principle binds E and H of the optical wave to δl through the cyclic permutation of their vector components (i,j),

$$\Delta E_i \Delta H_j \geq \hbar c^2 / 2\delta l^4. \quad (3)$$

As volumes smaller than the wavelength are probed, measurements of optical energy become uncertain, highlighting the difficulty with performing measurements in this regime.

Box 2
Surface plasmon length scales

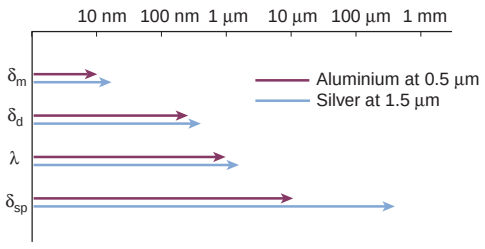

There are three characteristic length scales that are important for SP-based photonics in addition to that of the associated light. The propagation length of the SP mode, δ_{SP}, is usually dictated by loss in the metal. For a relatively absorbing metal such as aluminium the propagation length 2 μm at a wavelength of 500 nm. For a low loss metal, for example, silver, at the same wavelength it is increased to 20 μm. By moving to a slightly longer wavelength, such as 1.55 μm, the propagation length is further increases towards 1 mm. The propagation length sets the upper size limit for any photonic circuit based on SPs. The decay length in the dielectric material, δ_d, is typically of the order of half the wavelength of light involved and dictates the maximum height of any individual features, and thus components, that might be used to control SPs. The ratio of δ_{SP}:δ_d thus gives one measure of the number of SP-based components that may be integrated together. The decay length in the metal, δ_m, determines the minimum feature size that can be used; as shown in the diagram, this is between one and two orders of magnitude smaller than the wavelength involved, thus highlighting the need for good control of fabrication at the nanometre scale. The combinations chosen give an indication of range from poor (Al at 0.5 μm) to good (Ag at 1.5 μm) SP performance.

Box 3
Surface plasmon bandgaps

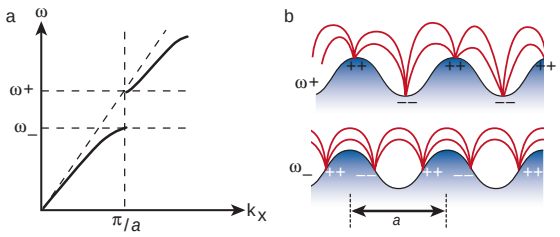

Periodic texturing of the metal surface can lead to the formation of an SP photonic bandgap when the period, *a*, is equal to half the wavelength of the SP, as shown in the dispersion diagram (**a**). Just as for electron waves in crystalline solids, there are two SP standing wave solutions, each with the same wavelength but, owing to their different field and surface charge distributions, they are of different frequencies. The upper frequency solution, ω_+, is of higher energy because of the greater distance between the surface charges and the greater distortion of the field, as shown schematically in **b**. SP modes with frequencies between the two band edges, ω_+ and ω_-, cannot propagate, and so this frequency interval is known as a stop gap. By providing periodic texture in two dimensions, SP propagation in all in-plane directions can be blocked, leading to the full bandgap for SPs. At the band edges the density of SP states is high, and there is a significant increase in the associated field enhancement.

This is not as serious a limitation as one might imagine, because, although we would often like to measure the optical energy (for which we need to know both the electric and magnetic field strengths), many optical interactions are dominated by just one of the fields, and so mapping just one of them on a subwavelength scale can provide invaluable new insights. For example, most PSTM tips provide images that are proportional to the mapping of the distribution of $|E|^2$ in the near-field zone[36]. Surprisingly, SPs with circular symmetry, sustained by a suitable metal coating of the tip, played a crucial role in the recent demonstration[37] that the distribution of $|H|^2$ associated with the optical wave can also be detected. Not only does this provide new possibilities for SPs, but it also enhances their role in such phenomena as the magneto-optic Kerr effect[38,39] in extending the realm in which SPs have important photonic applications.

Near-field mapping techniques such as PSTM have been essential for the development of SP devices such as waveguides and other components. For example, they were used to map the field distribution associated with an SP waveguide based on a metal stripe[40–42] that is illustrated in Fig. 1. Other strategies for waveguiding have also been explored, for example, using a well defined stripe defect on a periodically modulated photonic surface, with the defect acting as a guide[43]. It was recently pointed out that SP waveguides can be obtained by exploiting roughness-induced Anderson localization, which inhibits SP propagation. In this case, waveguides are formed by channels flattened across an otherwise rough metal film[44]. Waveguides can also be made of aligned metal (for example, gold) nanoparticles: a recent PSTM study has demonstrated the feasibility of laterally squeezing the optical near field by coupling localized SPs of an ensemble of linearly aligned gold nanoparticles[45], which suggests another approach to SP guiding[46].

By making use of advanced lithographic techniques to texture the

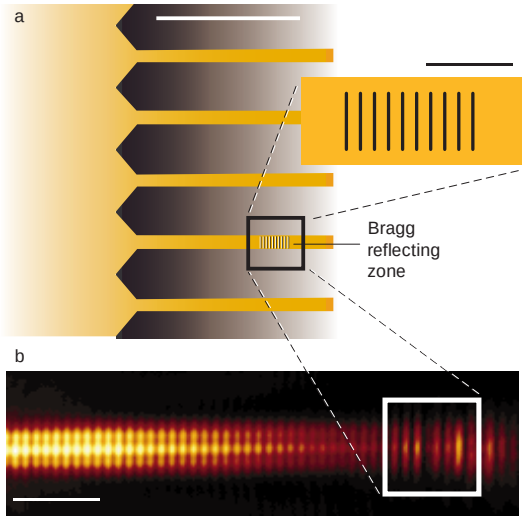

Figure 3 Surface plasmon Bragg reflector. **a**, An example of integration involving a Bragg reflector on a SP waveguide is provided by carving a series of slots with suitable sizes and separations in a gold stripe supported on a glass substrate, as shown on the SEM image (**a**) of a stripe similar to the one introduced in Fig. 1 (courtesy of E. Devaux, Université Louis Pasteur, France, and J. C. Weeber, Université de Bourgogne, France). White bar, 30 μm; black bar, 2.5 μm. The incident SP, with three maxima (see Fig. 1), is excited by total internal reflection illumination as described in the legend of Fig. 1. The SP propagates from the left to the right until it reaches the Bragg reflecting zone (indicated by the blue squares). The mirror effect is clearly observed in the PSTM image (**b**) as the interference between incident and reflected SPs. To the right of the mirror zone, the intensity falls dramatically to a value not detectable by the PSTM tip. Bar, 2.5 μm.

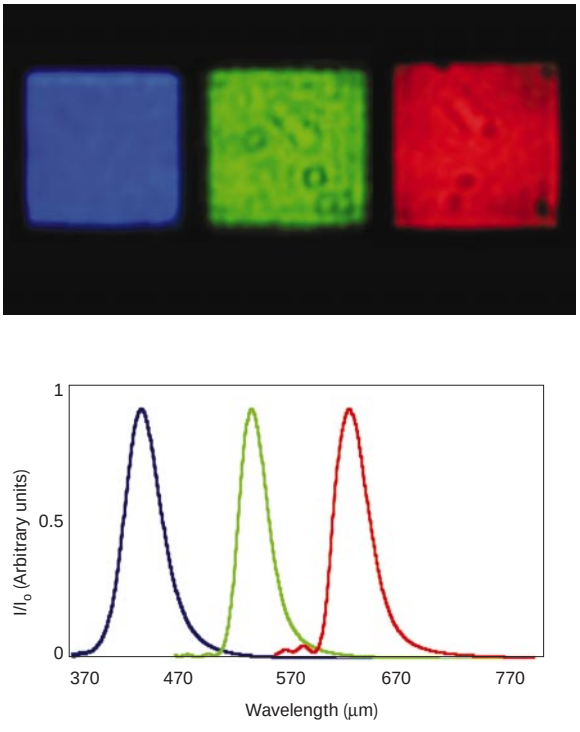

Figure 4 Normal incidence transmission for subwavelength holes. Normal incidence transmission images (top) and spectra (bottom) for three square arrays of subwavelength holes. For the blue, green and red arrays, the periods were 300, 450 and 550 nm, respectively, the hole diameters were 155, 180 and 225 nm and the peak transmission wavelengths 436, 538 and 627 nm. The arrays were made in a free standing 300 nm thick silver film (courtesy of A. Degiron, Université Louis Pasteur, France). Only the lowest order peak ($i,j = 0.1$ in equation (4)) of the spectrum of each array is shown as it dominates the colour seen.The figure shows that nanostructures can control the resonant wavelength of SP phenomena.

metal surface with protrusions, slits or holes, lenses and mirrors for SPs may be integrated into circuits not only on an extended thin film[18] but also directly on a finite-width stripe. An example of such a structure is shown in Fig. 3, where a Bragg reflector for SP modes is demonstrated. Although not yet fully optimized, these early demonstrations strengthen the prospect for SP-based photonic elements.

Hole arrays

The demonstration of enhanced transmission through periodic arrays of subwavelength holes in optically thick metallic films has sparked new interest in SPs[47–50]. Not only is the transmission much higher than expected from classic diffraction theory, it can be greater than the percentage area occupied by the holes, implying that even the light impinging on the metal between the holes can be transmitted. In other words, the whole periodic structure acts like an antenna in the optical regime, nicely demonstrating the benefits that SP modes can provide. The transmission spectra of hole arrays display peaks that can be tuned by adjusting the period and the symmetry as shown in Fig. 4. For a square array of period a_0, the peaks λ_{max} in the normal incidence transmittance spectra can be identified approximately from the dispersion relation (equation (1)), and they are given by:

$$\lambda_{max}\sqrt{i^2+j^2} \simeq a_0\sqrt{\frac{\varepsilon_m\varepsilon_d}{\varepsilon_m+\varepsilon_d}} \qquad (4)$$

where indices i and j are the scattering orders from the array[48].

For a free-standing hole array, incident light is diffracted/scattered by the array, producing evanescent waves that tunnel through the holes, resulting in a small but finite amplitude on the far side of the array. Here the evanescent waves are again diffracted/scattered; the interference of the resulting waves produces the light that propagates away from the structure. Equation (4) acts as a starting point in analysing the transmission spectrum, a spectrum that is more accurately determined by taking into account these diffraction/interference effects[51–55]. SPs act to enhance the fields associated with the evanescent waves, thus producing a way to increase the transmittance. When the metal film is thin enough, this tunneling may become resonant because the SP modes on the two surfaces can overlap and interact via the holes[49–51]. Interestingly, photon entanglement can be preserved or lost upon transmission through a hole, depending on the experimental conditions[56].

Single apertures

Individual subwavelength apertures can also exhibit enhanced transmission when surrounded by a periodic structure that harvests the incident light. If such nanostructure is added to the output side of the film then, remarkably, the emerging light can be beamed rather than diffracted. In addition, the light is mostly re-emitted from a very small area surrounding the aperture[57]. This suggests that a well directed source of light can be generated using a subwavelength aperture, an exciting development that is being pursued as a source for a variety of optical technologies, including high-density magneto-optic data storage. A theoretical treatment[58] shows that just a few well designed features around the exit of a slit aperture can give rise to beaming, as confirmed recently in the microwave region[59] and shown vividly in the numerical simulation presented in Fig. 5.

In the single hole and hole array structures described above, the holes do not support any propagating modes, that is, the diameter of the hole is smaller than $\lambda/2$ (half the wavelength of the light that is transmitted), and tunnelling is necessarily part of the transmission mechanism. However, when the aperture is larger than $\lambda/2$ in at least one dimension, such as a slit, then the aperture can support propagating modes[60–62]; the slit can even be wrapped up in the form of an annulus[63]. For instance, investigations of the transmission spectrum of periodic slit arrays reveal that both the slit modes and the modes caused by the periodic modulation of the surface (standing wave surface modes) play a role. In the case of a single slit surrounded by linear grooves, the transmission spectrum is dominated by the modes caused by the periodic groove structure, although other modes play an important role[64].

Future directions

In addition to their use in photonic circuits, SPs are being explored for other photonic technologies, notably the generation of light. A particular example is that of the organic light-emitting diode. Here excitons are produced by injection of charge into a semi-conducting organic layer that is typically only 100 nm thick. The close proximity of the excitons to the metallic cathode used to inject electrons means that much of the power that would otherwise have been radiated is in fact lost to SP modes on the cathode surface[65–68], thus detracting from device efficiency. Managing and, if necessary, recovering this power through the use of a periodic nanostructure is likely to be important for many future device designs, especially for high-efficiency, long-life and full-colour devices. The inverse process, that of using SPs to enhance the absorption of light, for example, in solar cells[69,70], is also of interest. SP modes have even been employed as the lasing mode in quantum cascade lasers[71].

To develop SP-based photonics, non-linear components such as switches will also be required. The unique properties of SPs give them some advantages in this respect. We mentioned that they are characterized by an evanescent, near field that is enhanced close to the surface. The use of SPs to enhance non-linear processes such as harmonic generation is well known[72–74], but it is only recently that experiments have been designed to look at how non-linear effects may be used to provide

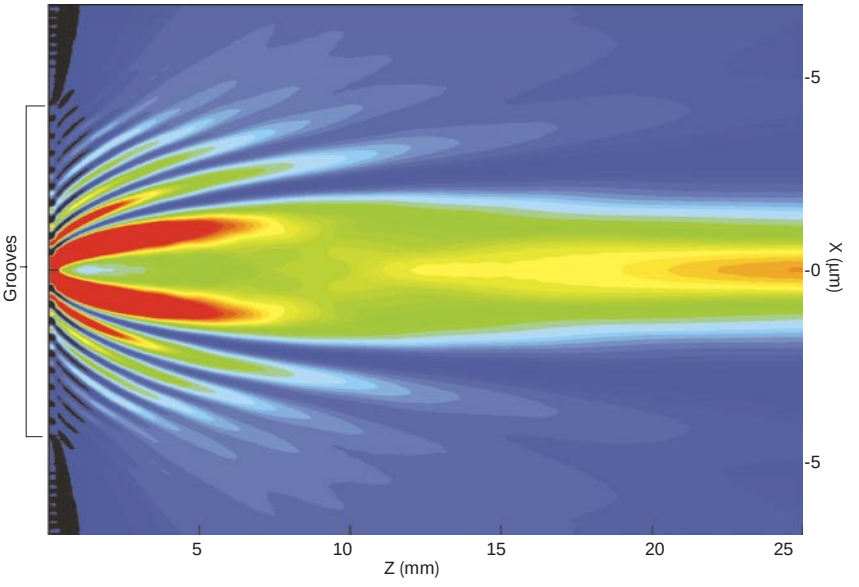

Figure 5 Calculated pattern of light emerging from a single slit surrounded by a finite array of grooves (courtesy of F. J. García-Vidal, Universidad Autonoma de Madrid, Spain) and L. Martín-Moreno (Universidad de Zaragoza, Spain). For this simulation there were 10 grooves on each side of the slit, each of width 40 nm and depth 100 nm. The groove period was 500 nm. The contour plot shows the spatial dependence of the component of the Poynting vector along the radial direction for a wavelength of 560 nm, corresponding to a spectral transmission maximum. Blue indicates low intensity (3×10^{-4}), and red high (1).

new elements for SP-based photonics[75]. This is an area in urgent need of further work.

SPs show great potential as a new class of subwavelength photonic devices; their particular attractions are their near-field character and their associated field enhancements. Nanoscale lithography enables researchers to explore the underlying science and has already led to proof-of-concept demonstrations, notably of waveguides, reflectors, beam splitters, enhanced transmission and beaming. Some of these components may find their way into the world of photonics as discrete elements. The greater dream of making a completely plasmonic circuit will require much further research. It is an exciting challenge that is stimulating activity around the world. □

doi:10.1038/nature01937

1. Ritchie, R. H. Plasma losses by fast electrons in thin films. *Phys. Rev.* **106,** 874–881 (1957).
2. Burstein, E. in *Polaritons* (eds Burstein, E. & De Martini, F.) 1–4 (Pergamon, New York, 1974).
3. Hecht, B., Bielefeldt, H., Novotny, L., Inouye, Y. & Pohl, D. W. Local excitation, scattering, and interference of surface plasmons. *Phys. Rev. Lett.* **77,** 1889–1892 (1996).
4. Pendry, J. Playing tricks with light. *Science* **285,** 1687–1688 (1999).
5. Kneipp, K. *et al*. Single molecule detection using surface-enhanced Raman scattering (SERS). *Phys. Rev. Lett.* **78,** 1667–1670 (1997).
6. Nie, S. M. & Emery, S. R. Probing single molecules and single nanoparticles by surface- enhanced Raman scattering. *Science* **275,** 1102–1106 (1997).
7. Homola, J., Yee, S. S. & Gauglitz, G. Surface plasmon resonance sensors: review. *Sensors Actuat. B* **54,** 3–15 (1999).
8. Kneipp, K., Kneipp, H., Itzkan, I., Dasari, R. R. & Feld, M. S. Surface enhanced Raman scattering and biophysics. *J. Phys. C* **14,** R597–R624 (2002).
9. Sambles, J. R., Bradbery, G. W. & Yang, F. Z. Optical-excitation of surface-plasmons - an introduction. *Contemp. Phys.* **32,** 173–183 (1991).
10. Kretschmann, E. & Raether, H. Radiative decay of nonradiative surface plasmons excited by light. *Z. Naturforsch. A* **23,** 2135–2136 (1968).
11. Otto, A. Exitation of nonradiative surface plasma waves in silver by the method of frustrated total reflection. *Z. Phys.* **216,** 398 (1968).
12. Ditlbacher, H. *et al*. Fluorescence imaging of surface plasmon fields. *Appl. Phys. Lett.* **80,** 404–406 (2002).
13. Ritchie, R. H., Arakawa, E. T., Cowan, J. J. & Hamm, R. N. Surface-plasmon resonance effect in grating diffraction. *Phys. Rev. Lett.* **21,** 1530–1533 (1968).
14. Wood, R. W. On a remarkable case of uneven distribution of light in a diffraction grating spectrum. *Phil. Mag.* **4,** 396 (1902).
15. Raether, H. Surface Plasmons (ed. Hohler, G.) (Springer, Berlin, 1988).
16. Moreland, J., Adams, A. & Hansma, P. K. Efficiency of light emission from surface plasmons. *Phys. Rev. B* **25,** 2297–2300 (1982).
17. Worthing, P. T. & Barnes, W. L. Efficient coupling of surface plasmon polaritons to radiation using a bi-grating. *Appl. Phys. Lett.* **79,** 3035–3037 (2001).
18. Ditlbacher, H., Krenn, J. R., Schider, G., Leitner, A. & Aussenegg, F. R. Two-dimensional optics with surface plasmon polaritons. *Appl. Phys. Lett.* **81,** 1762–1764 (2002).
19. Cregan, R. F. *et al*. Single-mode photonic band gap guidance of light in air. *Science* **285,** 1537–1539 (1999).
20. Kitson, S. C., Barnes, W. L. & Sambles, J. R. A full photonic band gap for surface modes in the visible. *Phys. Rev. Lett.* **77,** 2670–2673 (1996).
21. Barnes, W. L., Preist, T. W., Kitson, S. C. & Sambles, J. R. Physical origin of photonic energy gaps in the propagation of surface plasmons on gratings. *Phys. Rev. B* **54**, 6227–6244 (1996).
22. Barnes, W. L., Kitson, S. C., Preist, T. W. & Sambles, J. R. Photonic surfaces for surface plasmon polaritons. *J. Opt. Soc. Am. A* **14,** 1654–1661 (1997).
23. Kreibig, U. & Vollmer, M. Optical properties of metal clusters (Springer, Berlin, 1995).
24. Special issue: Optical Properties of Nanoparticles. *Appl. Phys. B* **73** (2001).
25. Haynes, C. L. & Van Duyne, R. P. Nanosphere lithography: A versatile nanofabrication tool for studies of size-dependent nanoparticle optics. *J. Phys. Chem. B* **105,** 5599–5611 (2001).
26. Sonnichsen, C. *et al*. Spectroscopy of single metallic nanoparticles using total internal reflection microscopy. *Appl. Phys. Lett.* **77,** 2949–2951 (2000).
27. Schultz, D. A. Plasmon resonant particles for biological detection. *Curr. Opin. Biotechnol.* **14,** 13–22 (2003).
28. Oldenburg, S. J., Genick, C. C., Clark, K. A. & Schultz, D. A. Base pair mismatch recognition using plasmon resonant particle labels. *Anal. Biochem.* **309,** 109–116 (2002).
29. Félidj, N. *et al*. Optimized surface-enhanced Raman scattering on gold nanoparticle arrays. *Appl. Phys. Lett.* **82,** 3095–3097 (2003).
30. Levi, S. A. *et al*. Fluorescence of dyes adsorbed on highly organized, nanostructured gold surfaces. *Chem.-a Eur. J.* **8,** 3808–3814 (2002).
31. Vargas-Baca, I. *et al*. Linear and nonlinear optical responses of a dye anchored to gold nanoparticles dispersed in liquid and polymeric matrixes. *Can. J. Chem.* **80**, 1625–1633 (2002).
32. Rechberger, W. *et al*. Optical properties of two interacting gold nanoparticles. *Opt. Commun.* **220,** 137–141 (2003).
33. Kottmann, J. P. & Martin, O. J. F. Retardation-induced plasmon resonances in coupled nanoparticles. *Opt. Lett.* **26,** 1096–1098 (2001).
34. García-Vidal, F. J. & Pendry, J. B. Collective theory for surface enhanced Raman scattering. *Phys. Rev. Lett.* **77,** 1163–1166 (1996).
35. Gresillon, S. *et al*. Experimental observation of localized optical excitations in random metal-dielectric films. *Phys. Rev. Lett.* **82,** 4520–4523 (1999).
36. Weeber, J. C. *et al*. Observation of light confinement effects with a near-field optical microscope. *Phys. Rev. Lett.* **77,** 5332–5335 (1996).
37. Devaux, E. *et al*. Local detection of the optical magnetic field in the near zone of dielectric samples. *Phys. Rev. B* **62,** 10504–10514 (2000).
38. Silva, T. J. & Schultz, S. A scanning near-field optical microscope for the imaging of magnetic domains in reflection. *Rev. Sci. Instr.* **67,** 715–725 (1996).
39. Hermann, C. *et al*. Surface-enhanced magneto-optics in metallic multilayer films. *Phys. Rev. B* **64,** 235422 (2001).
40. Kottmann, J. P., Martin, O. J. F., Smith, D. R. & Schultz, S. Plasmon resonances of silver nanowires with a nonregular cross section. *Phys. Rev. B* **64,** 5402 (2001).
41. Weeber, J. C., Dereux, A., Girard, C., Krenn, J. R. & Goudonnet, J. P. Plasmon polaritons of metallic nanowires for controlling submicron propagation of light. *Phys. Rev. B* **60,** 9061–9068 (1999).
42. Weeber, J. C. *et al*. Near-field observation of surface plasmon polariton propagation on thin metal stripes. *Phys. Rev. B* **64,** 045411 (2001).
43. Bozhevolnyi, S. I., Erland, J., Leosson, K., Skovgaard, P. M. W. & Hvam, J. M. Waveguiding in surface plasmon polariton band gap structures. *Phys. Rev. Lett.* **86,** 3008–3011 (2001).
44. Bozhevolnyi, S. I., Volkov, V. S. & Leosson, K. Localization and waveguiding of surface plasmon polaritons in random nanostructures. *Phys. Rev. Lett.* **89,** 186801 (2002).
45. Krenn, J. R. *et al*. Squeezing the optical near-field zone by plasmon coupling of metallic nanoparticles. *Phys. Rev. Lett.* **82,** 2590–2593 (1999).
46. Maier, S. A. *et al*. Local detection of electromagnetic energy transport below the diffraction limit in metal nanoparticle plasmon waveguides. *Nat. Mat.* **2,** 229–232 (2003).

47. Ebbesen, T. W., Lezec, H. J., Ghaemi, H. F., Thio, T. & Wolff, P. A. Extraordinary optical transmission through sub-wavelength hole arrays. *Nature* **391,** 667–669 (1998).
48. Ghaemi, H. F., Thio, T., Grupp, D. E., Ebbesen, T. W. & Lezec, H. J. Surface plasmons enhance optical transmission through subwavelength holes. *Phys. Rev. B* **58,** 6779–6782 (1998).
49. Krishnan, A. *et al*. Evanescently coupled resonance in surface plasmon enhanced transmission. *Opt. Commun.* **200,** 1–7 (2001).
50. Degiron, A., Lezec, H. J., Barnes, W. L. & Ebbesen, T. W. Effects of hole depth on enhanced light transmission through subwavelength hole arrays. *Appl. Phys. Lett.* **81,** 4327–4329 (2002).
51. Martín-Moreno, L. *et al*. Theory of extraordinary optical transmission through subwavelength hole arrays. *Phys. Rev. Lett.* **86,** 1114–1117 (2001).
52. Bonod, N., Enoch, S., Li, L., Popov, E. & Nevière, M. Resonant optical transmission through thin metallic films with and without holes. *Opt. Expr.* **11,** 482–490 (2003).
53. Vigoureux, V. M. Analysis of the Ebbesen experiment in the light of evanescent short range diffraction. *Opt. Commun.* **198,** 257–263 (2001).
54. Salomon, L., Grillot, F. D., Zayats, A. V. & de Fornel, F. Near-field distribution of optical transmission of periodic subwavelength holes in a metal film. *Phys. Rev. Lett.* **86,** 1110–1113 (2001).
55. Darmanyan, S. A. & Zayats, A. V. Light tunneling via resonant surface plasmon polariton states and the enhanced transmission of periodically nanostructured metal films. *Phys. Rev. B* **67,** 035424 (2003).
56. Altewischer, E., van Exter, M. P. & Woerdman, J. P. Plasmon-assisted transmission of entangled photons. *Nature* **418,** 304–306 (2002).
57. Lezec, H. J. et al. Beaming light from a subwavelength aperture. *Science* **107,** 1895 (2002).
58. Martín-Moreno, L., Garcia-Vidal, F. J., Lezec, H. J., Degiron, A. & Ebbesen, T. W. Theory of highly directional emission from a single sub-wavelength aperture surrounded by surface corrugations. *Phys. Rev. Lett.* **90,** 167401 (2003).
59. Hibbins, A. P., Sambles, J. R. & Lawrence, C. R. Gratingless enhanced microwave transmission through a subwavelength aperture in a thick metal plate. *Appl. Phys. Lett.* **81,** 4661–4663 (2002).
60. Porto, J. A., García-Vidal, F. J. & Pendry, J. B. Transmission resonances on metallic gratings with very narrow slits. *Phys. Rev. Lett.* **83,** 2845–2848 (1999).
61. García-Vidal, F. J. & Martín-Moreno, L. Transmission and focusing of light in one-dimensional periodically nanostructured metals. *Phys. Rev. B* **66,** 155412 (2002).
62. Barbara, A., Quemerais, P., Bustarret, E. & Lopez-Rios, T. Optical transmission through subwavelength metallic gratings. *Phys. Rev. B* **66,** 161403 (2002).
63. Baida, F. I. & Van Labeke, D. Light transmission by subwavelength annular aperture arrays in metallic films. *Opt. Commun.* **209,** 17–22 (2002).
64. García-Vidal, F. J., Lezec, H. J., Ebbesen, T. W. & Martín-Moreno, L. Multiple paths to enhance optical transmission through a single subwavelength slit. *Phys. Rev. Lett.* **90,** 213901 (2003).
65. Weber, W. H. & Eagen, C. F. Energy transfer from an excited dye molecule to the sureface plasmons of an adjacent metal. *Opt. Lett.* **4,** 236–238 (1979).
66. Pockrand, I., Brillante, A. & Möbius, D. Nonradiative decay of excited molecules near a metal surface. *Chem. Phys. Lett.* **69,** 499–504 (1980).
67. Barnes, W. L. Fluorescence near interfaces: the role of photonic mode density. *J. Mod. Opt.* **45,** 661–699 (1998).
68. Hobson, P. A., Wedge, S., Wasey, J. A. E., Sage, I. & Barnes, W. L. Surface plasmon mediated emission from organic light emitting diodes. *Adv. Mat.* **14,** 1393–1396 (2002).
69. Andrew, P., Kitson, S. C. & Barnes, W. L. Surface plasmon energy gaps and photoabsorption. *J. Mod. Opt.* **44,** 395–406 (1997).
70. Westphalen, M., Kreibig, U., Rostalski, J., Luth, H. & Meissner, D. Metal cluster enhanced organic solar cells. *Sol. Energy Mat. Sol. Cells* **61,** 97–105 (2000).
71. Tredicucci, A. *et al*. Single-mode surface-plasmon laser. *Appl. Phys. Lett.* **76,** 2164–2166 (2000).
72. Coutaz, J. L., Neviere, M., Pic, E. & Reinisch, R. Experimental study of surface-enhanced second-harmonic generation on silver gratings. *Phys. Rev. B* **32,** 2227–2232 (1985).
73. Quail, J. C. & Simon, H. J. Second-harmonic generation with phase-matched long-range and short-range surface plasmons. *J. Appl. Phys.* **56,** 2589–2591 (1984).
74. Tsang, T. Y. F. Surface-plasmon-enhanced third-harmonic generation in thin silver films. *Opt. Lett.* **21**, 245–247 (1996).
75. Smolyaninov, I. I., Zayats, A. V., Gungor, A. & Davis, C. C. Single-photon tunneling via localized surface plasmons. *Phys. Rev. Lett.* **88,** 187402 (2002).